Cell Reports, Volume *38*

Supplemental information

Labeling of heterochronic ribosomes reveals C1ORF109 and SPATA5 control a late step in human ribosome assembly

Chunyang Ni, Daniel A. Schmitz, Jeon Lee, Krzysztof Pawłowski, Jun Wu, and Michael Buszczak

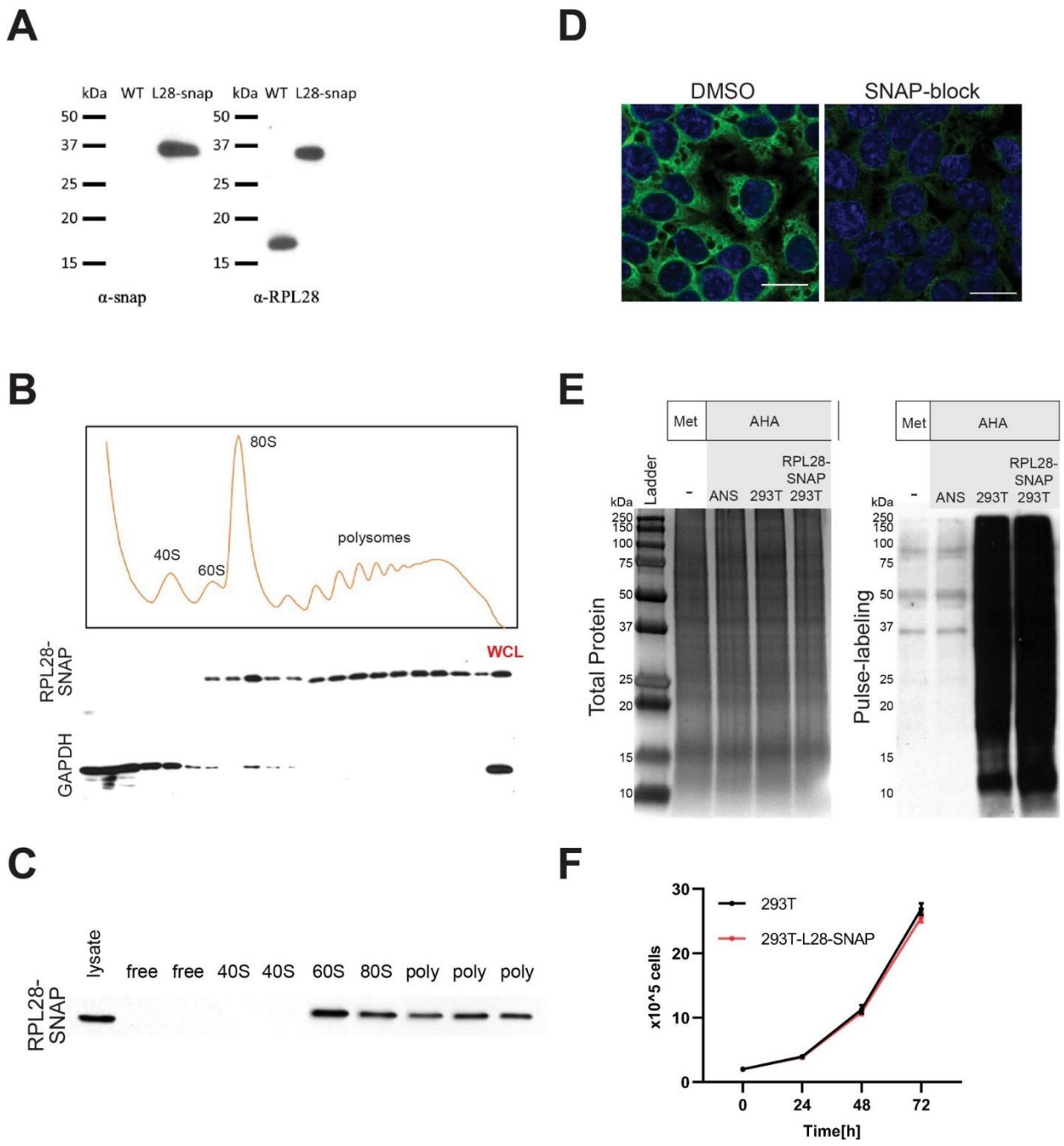

Figure S1. Generation of cell lines carrying SNAP-tagged RPL28. Related to Figure 1. (A) Western blots of control HEK293T cells and cells carrying a SNAP-tag at the endogenous RPL28 locus probed with the indicated antibodies. (B) Distribution of SNAP-tagged RPL28 across a sucrose gradient shows the protein co-fractionates with the 60S subunit, 80S monosome, and polysomes as expected. GAPDH is included as a free control. WCL, whole-cell lysate. (C) Distribution of SNAP-tagged RPL28 from human ESCs across a sucrose gradient. (D) HEK293T cells expressing SNAP-tagged RPL28 were treated with DMSO or unconjugated benzylguanine (SNAP-block) and then labeled with benzylguanine-Oregon green for 30 minutes. Treatment with

benzylguanine “blocks” the labeling of pre-existing ribosomes. Scale bars represent 20µm. (E) Wild type HEK293T or HEK293T-RPL28-SNAP cells were pulse-labeled with Methionine, or AHA, or AHA with anisomycin (ANS) for 3h. Protein extract was labeled with biotin and analyzed by blotting with HRP-Streptavidin. The unfixed total protein staining demonstrates equal loading. (F) Wildtype HEK293T or HEK293T-RPL28-SNAP cells were seeded at 2.0x10^5 cells and were counted 24, 48, 72h after seeding. (n=6 counts per time point). Mean ± S.E.M. is shown.

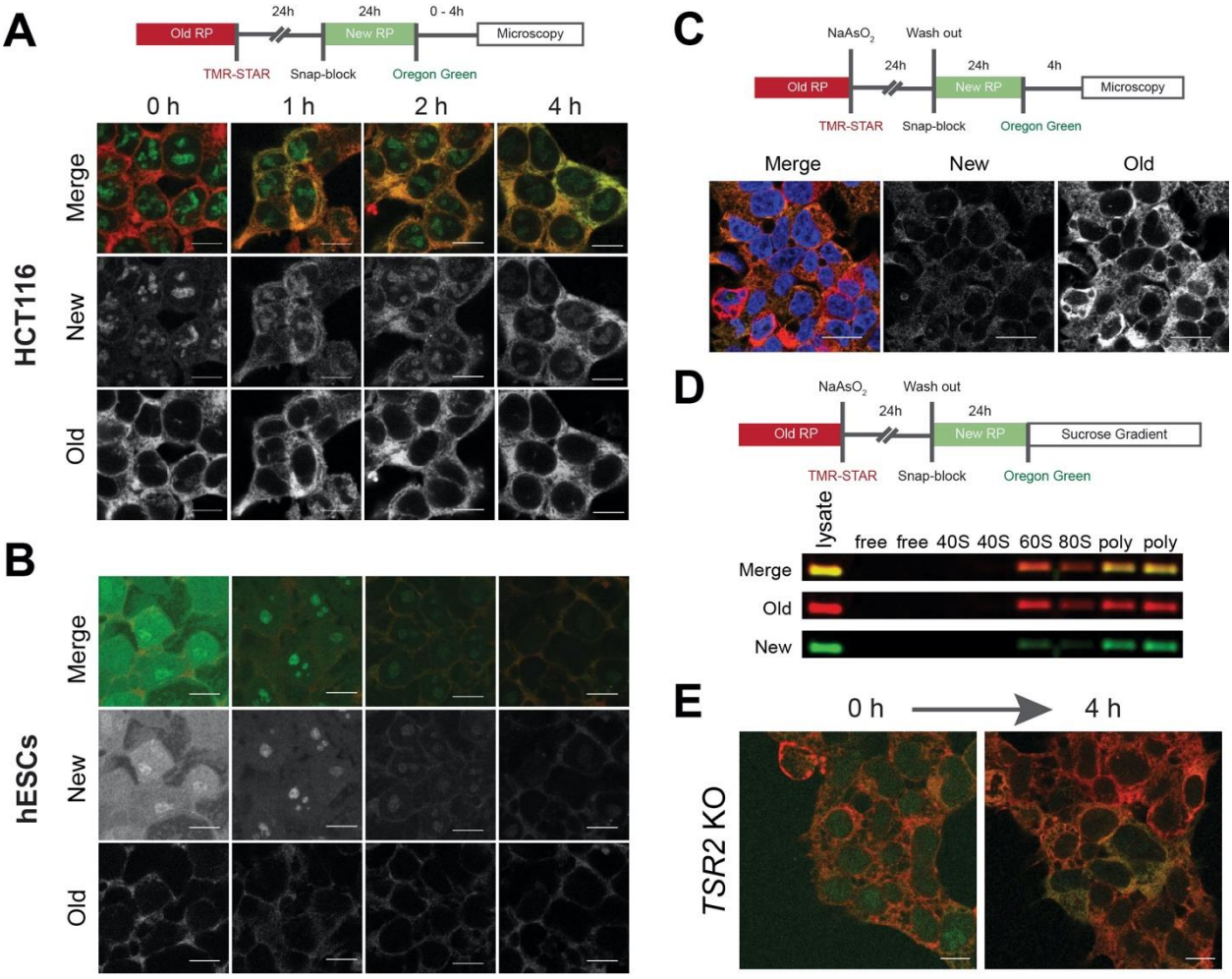

Figure S2. Pulse-chase experiments examining the distribution of old and new RPL28 in HCT116 and H9 cells. (Related to Figure 1) (A) HCT116 and (B) hESCs pulse-labeled as indicated in the schematic. All imaging was conducted using the same parameters. Scale bars represent 10 μm. (C) The distribution of old and new ribosomes in HEK293T cells treated with $NaAsO_2$. Scale bars represent 20 μm. (D) 60S subunits present during $NaAsO_2$ treatment accumulated in the 60S and polysome fractions, whereas ribosomes generated after the treatment are more readily recruited into the polysome fractions. (E) Cells carrying SNAP-tagged RPL28 transduced with sgRNAs targeting TSR2 and subjected to pulse-labeling.

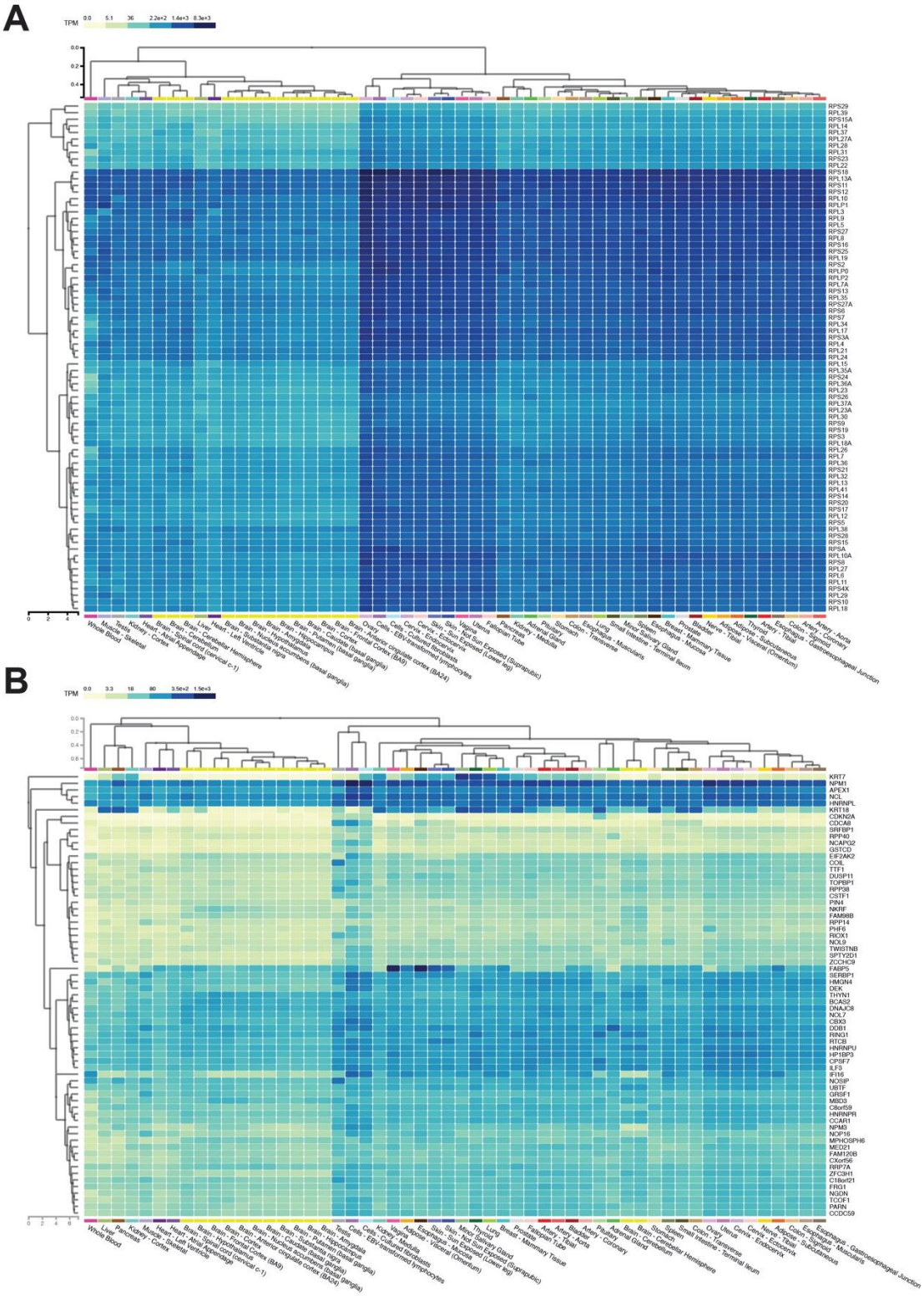

Figure S3. GTex expression analysis of ribosome proteins and ribosome assembly factors. (Related to Figure 1) (A) Heat map of mRNA expression levels of all 80 human ribosomal proteins across the indicated tissues. (B) Heat map of mRNA expression levels of ribosome biogenesis factors not found in yeast (Tafforeau *et al.*, 2013).

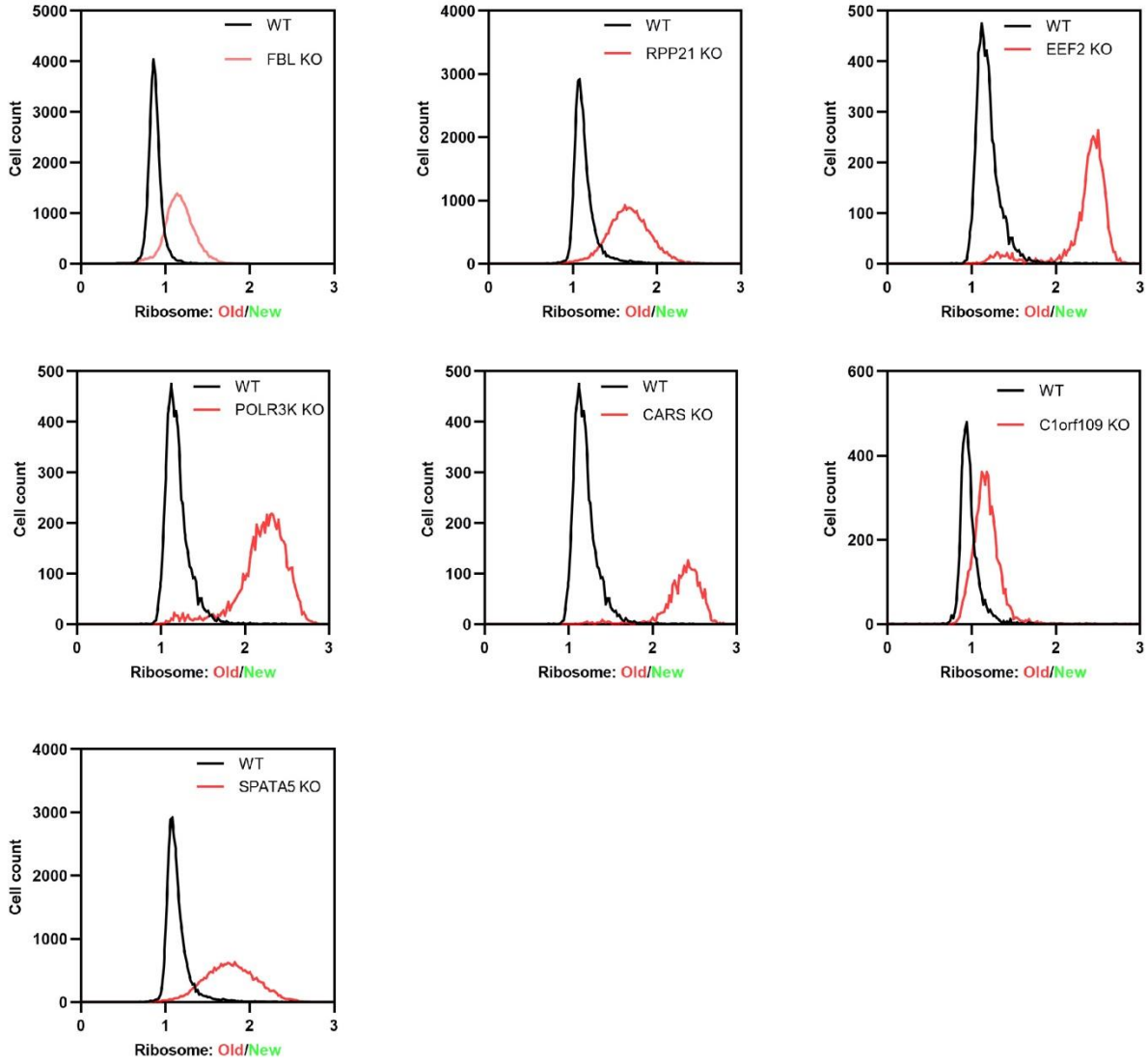

Figure S4. Flow cytometry validation of genes identified in the primary screen. (Related to Figure 2). Flow cytometry validation of HEK293T cells labeled for new and old ribosomes transduced with sgRNAs targeting the indicated gene (red) compared to control cells receiving an empty vector (black). (n>10,000 cells per condition). The ratio of old to new ribosomes is plotted on each x-axis.

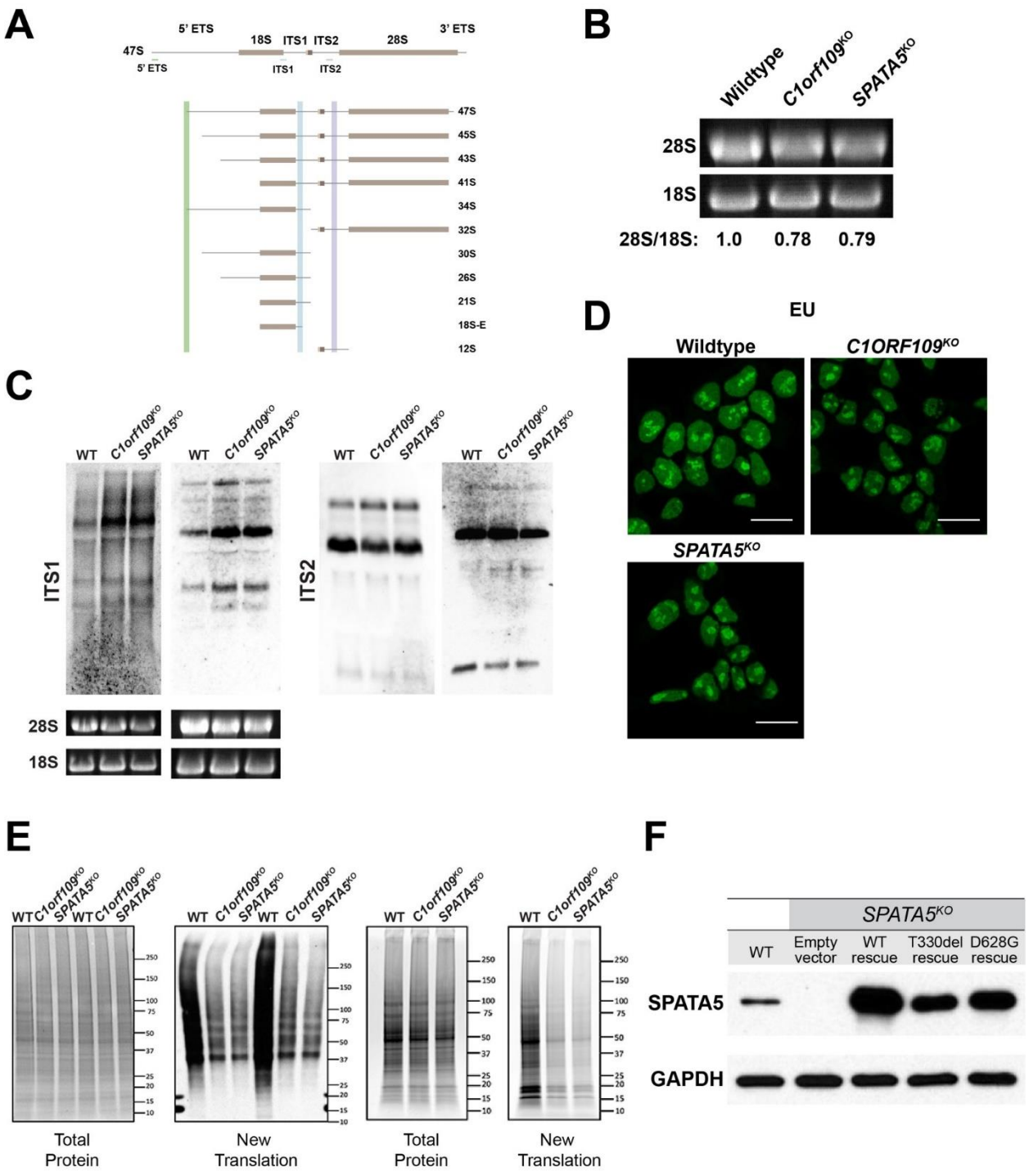

Figure S5. Loss of *C1ORF109* and *SPATA5* disrupts ribosome maturation. (Related to Figure 3 and Figure 5). (A) Schematic of rRNA processing intermediates (based on *(Tafforeau et al., 2013)*) (B) Levels of mature 28S and 18S from wildtype, *C1ORF109*^{KO} and *SPATA5*^{KO} cells. Loading is the same for northern blots presented in Fig. 4. (C) Representative repeats of northern blots probed for ITS1 and ITS2. (D) Cells transduced with sgRNAs targeting *C1ORF109* and *SPATA5* pulse-labeled with EU (green). Loss of *C1ORF109* and *SPATA5* results in a reduction of EU labeling within nucleoli relative to control cells. Scale bars represent 20 μm. (E) Representative repeats

of AHA pulse labeling experiments comparing new protein synthesis between control cells and *C1ORF109*^{KO} and *SPATA5*^{KO} cells. (E) Western blot analysis probed for SPATA5 and GAPDH showing the expression levels of endogenous SPATA5 compared to the expression of the three different SPATA5 transgenes.

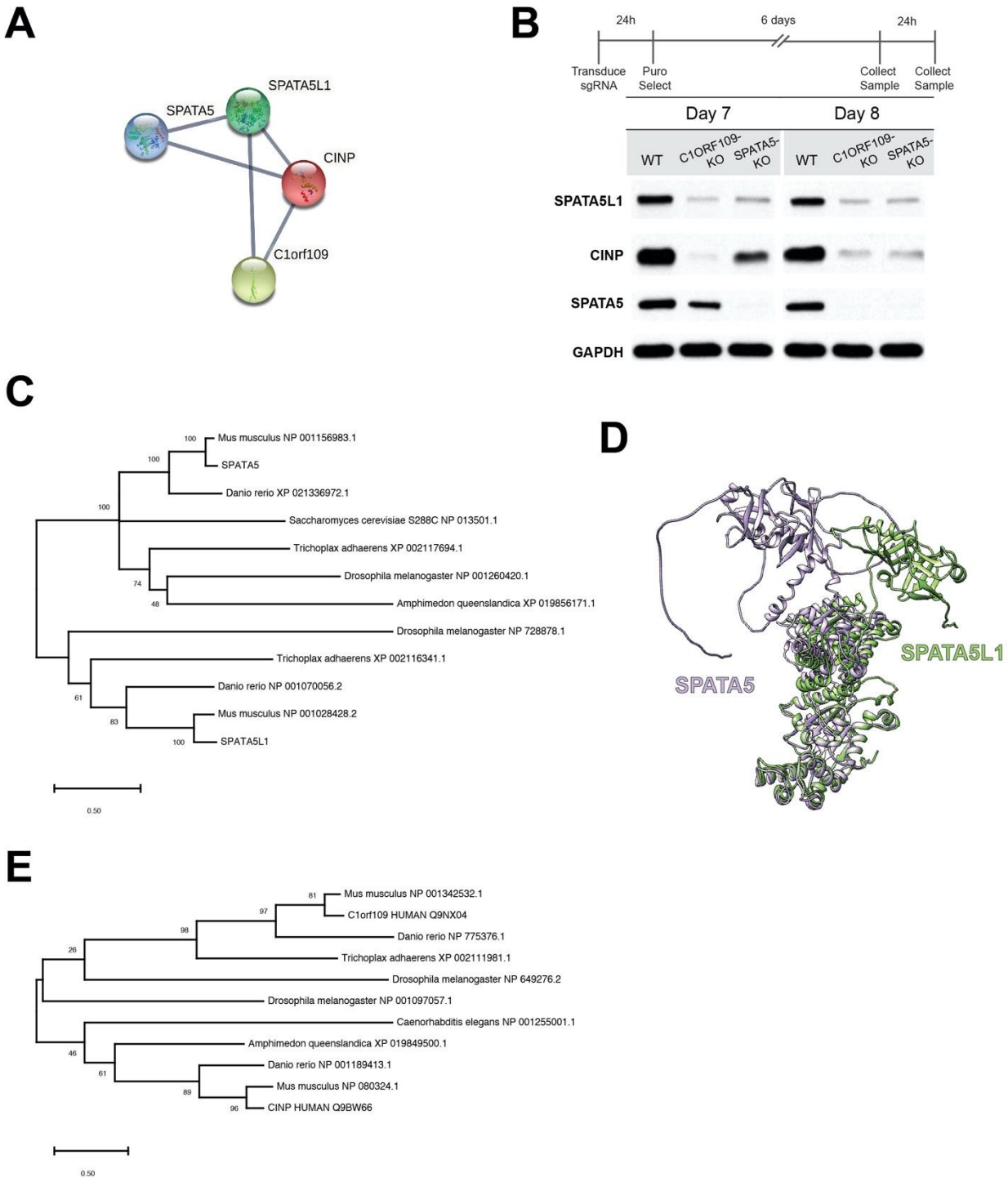

Figure S6. SPATA5 and C1ORF109 interact with CINP and SPATA5L1. (Related to Figure 6). (A) String analysis indicates that C1ORF109, SPATA5, SPATA5L1 and CINP likely associate with one another (Szklarczyk *et al.*, 2019). (B) Western blot reveals that loss of *C1ORF109* or *SPATA5* results in decreased levels of SPATA5L1 and CINP. (C) Phylogenetic trees of selected SPATA5 and SPATA5L1 homologs. Maximum likelihood phylogenetic analysis applied (MEGA X), branch support values shown (500 bootstrap replicates). Branch lengths shown as the numbers of substitutions per site. NCBI identifiers of sequences shown. (D) Matchmaker structural alignment of Alphafold

predictions of SPATA5 and SPATA5L1. (E) Phylogenetic trees of C1ORF109 and CINP homologs. Details same as (C).

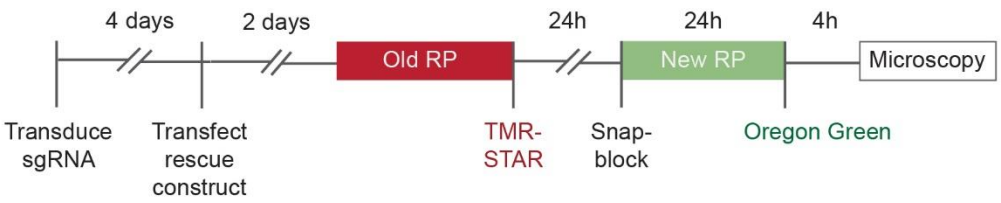

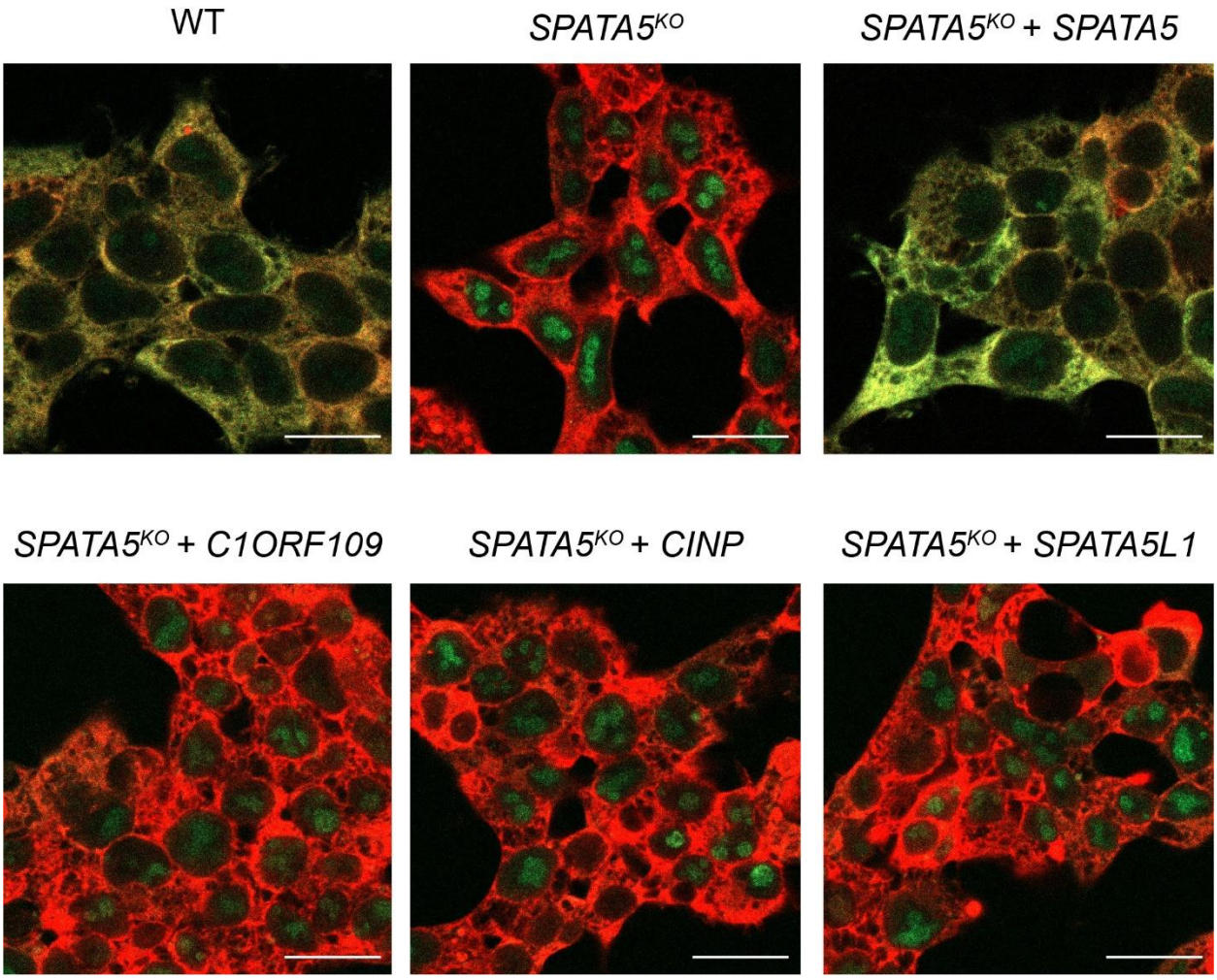

Figure S7. *SPATA5L1*, *CINP*, and *C1ORF109* transgenes do not rescue the ribosome biogenesis defects on *SPATA5*^{KO} cells. (Related to Figure 6). (A) Control and *SPATA5*^{KO} HEK293T cells transfected with wildtype *SPATA5*, *CINP*, *C1ORF109* and *SPATA5L1* rescue constructs stained for old and new ribosomes according to the schematic. Scale bars represent 20 µm.